

Grafting of Swelling Clay Materials with 3-aminopropyltriethoxysilane

Hongping He ^{a,b}, Jannick Duchet ^{a,*}, Jocelyne Galy ^a, Jean-François Gerard ^a

^a Laboratoire des Matériaux Macromoléculaires/IMP, UMR 5627 - IMP, INSA Lyon, Bât. Jules Verne, 20 avenue A. Einstein, 69621 Villeurbanne, France

^b Guangzhou Institute of Geochemistry, Chinese Academy of Sciences, Wushan, Guangzhou 510640, China

This is the authors' version of a paper that was later published as

He, Hongping and Duchet, Jannick and Galy, Jocelyne and Gerard, Jean-François (2005) Grafting of Swelling Clay Materials with 3-aminopropyltriethoxysilane. *JOURNAL OF COLLOID AND INTERFACE SCIENCE* 288(1):171-176.

Abstract

The grafting reaction between a trifunctional silylating agent and two kinds of 2:1 type layered silicates was studied using FTIR, XRD, TGA and ²⁹Si CP/MAS NMR. XRD patterns clearly indicate the introduction of 3-aminopropyltriethoxysilane (γ -APS) into the clay interlayer. In the natural montmorillonite, γ -APS adopts a parallel-bilayer while it adopts a parallel-monolayer arrangement in the synthetic fluorohectorite. These different silane arrangements have a prominent effect on the mechanism of the condensation reaction within the clay gallery. In natural montmorillonite, the parallel-bilayer arrangement of γ -APS results in bidentate (T^2) and tridentate (T^3) molecular environment while the parallel-monolayer arrangement leads to monodentate (T^1), as indicated by ²⁹Si CP/MAS NMR spectra. This study demonstrates that the silylation reaction and the interlayer microstructure of the grafting products strongly depend on the original clay materials.

Keywords: 3-aminopropyltriethoxysilane; natural montmorillonite; synthetic fluorohectorite; grafting; X-ray diffraction; thermogravimetric analysis; ²⁹Si CP/MAS NMR

I. Introduction

During the past 50 years, there has been an increased interest in the synthesis of nanocomposite materials by embedding nanosized inorganic particles into polymers [1]. Since the optical, thermal, rheological and mechanical properties of these materials strongly depend on the techniques used for their elaboration, a variety of synthesis strategies have been reported with the aim to control the dispersion of the inorganic component within the polymer matrix at the nanoscale. Among the wide range of nanostructured materials, effort has more recently focused on the elaboration of polymer/layered silicate nanocomposites.

The application of layered silicate relies on their ion exchange property and swelling ability. Access of guest molecule to host matrix could be a rate limiting step in the intercalation reaction of swelling clays. Especially, when guest molecules are highly hydrophobic and bulky, they would have a low possibility to approach hydrophilic reaction site. This kind of organic molecules is difficult to be intercalated into hydrophilic clays by the conventional ion exchange methods that employ the clay suspension with a single solution phase. Recently, their potentials have been tremendously expanded by the intercalation of a variety of biologically active organic substances [2-5]. Hydrophobic modification of the clay intra-surface allows many hydrophobic guest molecules to be easily intercalated.

More recently, some studies have demonstrated that the interaction between hydrophobic molecule and clay surface could be greatly enhanced by simple grafting of hydrophobic groups onto the layer surface [6,7]. In the previous studies of the interaction between silane and swelling clay materials, three basic models (interlayer, external surface and “broken” edge grafting) have been proposed. The interlayer grafting happens within the clay gallery and results in the prominent increase of the basal spacing of the clay [8-10]. The intercalation and silylation convert the hydrophilic interlayer surface to an organophilic surface. For the external surface [7] and “broken” edge [6] graftings, the silylation occurs on the external surface and “broken” edge, separately. The former has no effect on the basal spacing of the used clay whereas the later increases the basal spacing based on the assumption that the silylation reaction produces silane polymers able to penetrate the external part of the interlaminar space and push the clay sheets apart [6]. The successful grafting greatly enhances the intercalation of bulky hydrophobic molecules into clay materials. Obviously, in these reports, the locations for silylating reactions are very different from each other. In addition, we find researchers paid great attention on the effect from silanes with different number of functional groups whereas little attention was paid on the effect from the used clay materials. Based on our knowledge about clay minerals, the mineralogical properties (for example, swelling ability, ion exchange property) have significant effects on the interaction between clays and other chemicals. Hence, in this study, grafting different clay materials with the same silylating agent was performed, to elucidate the effect of clay minerals on the silylating reaction.

Among the various swelling clay materials, synthetic fluorohectorite (SOMASIF ME100) and natural montmorillonite (OPTIGEL-757) are the most widely used in the

synthesis of polymer/layered silicate nanocomposites. However, as far as is known, no study has been performed on these two clay materials grafted with silane. It is of high importance for synthesis of polymer/layered silicate nanocomposites and/or improvement of their properties.

In this work, we report the grafting of two 2:1 type swelling clay materials with a trifunctional silylating agent (3-aminopropyltriethoxysilane) and the characterization of the resultant products using FTIR, XRD, TGA and ^{29}Si CP/MAS NMR. The aim of this work is to elucidate the effect of clay materials on the silylation reaction and the interlayer microstructure of the grafting products. This is a strategic step for synthesis of polymer/layered silicate nanocomposites.

II. Experimental

1. Materials

Two kinds of 2:1 type swelling clay materials, SOMASIF ME100 (ME) and OPTIGEL-757 (NANOFIL) were used in this study. SOMASIF ME100 (ME) is a synthetic fluorohectorite produced by CO-OP Chemical Co., Japan. The cation exchange capacity (CEC) of ME is 70 meq/100g, and its interlayer spacing is 0.96 nm. Its structural formula can be expressed as $\text{Na}_{2x}\text{Mg}_{3.0-x}\text{Si}_4\text{O}_{10}(\text{F}_y\text{OH}_{1-y})_2$, ($x = 0.15-0.5$, $y = 0.8-1.0$). OPTIGEL-757 (NANOFIL) is a kind of natural montmorillonite provided by SÜD-CHEMIE Co., Germany and its formula is $\text{Na}_{0.19}\text{K}_{0.20}\text{Ca}_{0.04}(\text{Mg}_{0.36}\text{Fe}_{0.10}\text{Al}_{1.44})\text{Si}_4\text{O}_{10}(\text{OH})_2$. The CEC of OPTIGEL-757 is 91 meq/100g. The trifunctional silylating agent (3-aminopropyltriethoxysilane, γ -APS), with a purity of 99% (from Aldrich), was used as received. The chemical formula of γ -APS is $\text{H}_2\text{N}(\text{CH}_2)_3\text{Si}(\text{OC}_2\text{H}_5)_3$. The two original clays, SOMASIF ME100 (synthetic fluorohectorite) and OPTIGEL-757 (natural montmorillonite), are denoted as H-0 and M-0, respectively.

2. Grafting process

The grafting reaction was carried out in a mixture of water/ethanol (25/75 by volume). 3 grams of γ -APS was first introduced into 1000 ml of the mixture of water/ethanol and the temperature was kept at 80 °C. Then, 10 grams of clay was added into the above-mentioned solution and the grafting reaction was realized, under shearing, during 5 hours at 80 °C. The reaction product was filtered and washed using the mixture of H_2O /ethanol for six times and dried at 80 °C for 6-8 hours. The resultant product was ground and placed in a sealed container for characterization. The grafted products prepared from H-0 and M-0 are denoted as H-2 and M-2, respectively.

3. Characterization

X-ray powder diffraction (XRD) analysis was performed on a Siemens D500 diffractometer equipped with a back monochromator and a copper cathode as the X-ray source ($\lambda=0.154$ nm). The basal spacings were calculated from the 2θ values using the EVA software.

Fourier transform infrared (FTIR) spectra using KBr pressed disk technique were

performed on a Nicolet SX2 Fourier transform infrared spectrometer. The spectra were collected for each measurement over the spectral range of 400-4000 cm^{-1} with a resolution of 4 cm^{-1} .

Thermogravimetric analysis (TGA) was performed on a TGA2950 thermobalance. Samples were heated from 30°C to 800°C for M-0 and M-2, and to 950 °C for H-0 and H-2 at a heating rate of 20°C/mn under helium atmosphere (25 ml/min) in order to quantify and distinguish the amount of silane in the resultant products of grafting reaction.

^{29}Si cross-polarization magic-angle-spinning nuclear-magnetic-resonance (CP/MAS NMR) spectra were gained on a Bruker DSX-300 spectrometer operating at 59.63 MHz. The contact time was 5 ms, the recycle delay 1 s, and the spinning rate 5 KHz. Tetramethylsilane (TMS) was used as the external reference.

III. Results and Discussion

A lot of previous studies [11,12] have shown that hydroxyl groups on the silica surface, resulted from hydrolysis, act as active sites in the grafting reaction between silane and silica. For 2:1 type layered silicates, they have a kind of “sandwiched” structure, i.e., one $\text{Al}(\text{Mg})\text{-O}_4(\text{OH})_2$ octahedral sheet binds with two Si-O tetrahedral sheets as shown in Figure 1. Since the extensively existing structural defects in the Si-O tetrahedral sheet and the layer edges with “broken” bonds, these sites will be active, similar to the Si atom environment in silica, and combine with silane during grafting reaction.

Figure 2 displays the FTIR spectra of M-0, M-2, H-0 and H-2. A weak and broad band at ca. 2936 cm^{-1} was recorded in the FTIR spectra of M-2 and H-2 (Fig. 2). This band corresponds to CH_2 stretching mode of γ -APS, indicating the existence of silane in the grafted products. The XRD patterns of the clay materials before and after grafting are shown in Figure 3. The basal spacings for M-0 and H-0 are 1.18 nm and 1.21 nm, respectively. After grafting reaction, the basal spacing is increased to 1.77 nm for M-2 and to 1.45 nm for H-2 (Fig. 3). The broad (001) reflection of H-2 and M-2 reflects the variety of the layer height in the grafted products. The increase of the basal spacing indicates that γ -APS has been intercalated into the gallery of the both clay materials. The estimated gallery heights for M-2 and H-2 are 0.81 nm and 0.49 nm. In the solution of water/ethanol mixture, silane is easy to hydrolyze [13] and this is also confirmed by our ^{29}Si MAS NMR spectrum (see below). After hydrolysis, the configuration of γ -APS is different from the original one and the height of the aminopropyl group is ca. 0.4 nm, similar to that of alkyl chain [14]. Accordingly, the gallery heights of 0.81 and 0.49 nm indicate the parallel-bilayer and parallel-monolayer arrangement of γ -APS within the galleries of M-2 and H-2, respectively. Since the grafting reaction conditions for M-2 and H-2 are identical, their different gallery heights reflect that the original clays have a significant effect on the gallery structure of the resultant products. In addition, our present study demonstrates that M-0 is more expandable than H-0 as shown by the XRD patterns of the grafted products.

Both of the DTG curves of H-0 and M-0 display two peaks at 47 and 901 °C for

H-0 and at 62 and 625 °C for M-0 (Fig. 4), corresponding to loss of the physically adsorbed water and dehydroxylation of clay, respectively. As shown by the TGA curve of H-0, there is not any weight loss during 200 – 600 °C. This means that H-0 does not undergo any thermally induced changes in this temperature range. However, for M-0, there is a slight weight loss (ca. 1 wt.%) in the range of 200 – 500 °C, possibly corresponding to the loss of the bonded H₂O within the gallery. The DTG curve of H-2 (Fig. 4) displays five peaks at 63, 209, 347, 426 and 550 °C, respectively. The peak at 63 °C corresponds to loss of the physically adsorbed water. As shown by TGA curve, H-0 is thermally stable in the temperature range of 200-600 °C. Hence, the weight loss in this region should be attributed to the evaporation and/or decomposition of silane. The peak at 209 °C corresponds to the physically adsorbed γ -APS while the peak around 550 °C to the decomposition of the grafted silane [15]. In addition, the peaks at 347 and 428 °C, similar to those derived from the decomposition of the intercalated cationic surfactants within the clay interlayer [16], should be attributed to the intercalated silane. For M-2, the DTG curve displays four peaks at ca. 62, 330, 426 and 535 °C, respectively. The peak at 62 °C corresponds to the loss of the physically adsorbed water while the peaks at 330 and 426 °C to the intercalated silane. However, the peak at ca. 625 °C corresponding to dehydroxylation in DTG curve of M-0 does not occur in the DTG curve of M-2. Hence, the broad peak at ca. 535 °C in the DTG curve of M-2 could be due to the co-occurrence of the decomposition of the chemically bound silane and the dehydroxylation of the clay. The TGA curves of the two used clays before and after grafting indicate that there are 6.0% and 6.9% (wt%) of γ -APS within the galleries of M-2 and H-2, respectively. This reflects that the quantity of silane within the gallery is not the key factor for their arrangement. Here, we can say that the used clay materials have a more prominent effect on the arrangement of silane within the gallery rather than the amount of silane.

²⁹Si CP/MAS NMR spectrum provides supporting evidence for the silylation of silane onto the clay surface. ²⁹Si CP/MAS NMR spectrum of M-0 (Fig. 5) displays two signals at –92.1 and –108.3 ppm, corresponding to Q³[Si(OSi)₃OM] (M stands for Al, Mg, et al.) and Q⁴[Si(OSi)₄], respectively [17]. The former is characteristic of Si atom in layered silicate while the later relates with Si atom in quartz, which is an impurity in the clays. There is no signal of Q² attributed to isolated silanol groups present at the silicate sheet edges. This is similar to those of montmorillonites reported in literature [17], but different from that of laponite, in which a signal of Q² was recorded [6]. After grafting, two additional ²⁹Si signals at –59.8 ppm and –66.7 ppm are recorded in ²⁹Si CP/MAS NMR spectrum of M-2 in addition to the two signals of Q³ and Q⁴ occurring in the ²⁹Si NMR spectrum of M-0. The two signals at –59.8 ppm and –66.7 ppm correspond to the units of T²[Si(OSi)₂(OR')R] (R = CH₂CH₂CH₂NH₂, R' = H or CH₂CH₃) and T³[Si(OSi)₃R], respectively [6,8-11,13]. This demonstrates the successful grafting γ -APS onto the clay surface. For H-0, ²⁹Si CP/MAS NMR spectrum displays a signal centered at –89.3 ppm, corresponding to Q³[Si(OSi)₃OM]. In the ²⁹Si CP/MAS NMR spectrum of H-2, a strong ²⁹Si signal at –43.6 ppm and a weak one at –53.0 ppm are recorded. The former corresponds to T¹[Si(OSi)(OH)₂R] and the later to T¹[Si(OSi)(OCH₂CH₃)₂R] [11]. The stronger

signal intensities of the $T^1[\text{Si}(\text{OSi})(\text{OH})_2\text{R}]$ unit suggests that most silane molecules have hydrolyzed in the solution of water/ethanol mixture. This conclusion supports our proposal about the silane arrangement within the gallery based on the XRD patterns. In addition, the co-existence of $T^1[\text{Si}(\text{OSi})(\text{OH})_2\text{R}]$ and $T^1[\text{Si}(\text{OSi})(\text{OCH}_2\text{CH}_3)_2\text{R}]$ units gives good explanation of the obviously broadened (001) reflection of H-2.

Our present study demonstrates that the intercalation of silane firstly happens during grafting reaction and the arrangement of the intercalated silane strongly depends on the properties of layered silicates. This is similar to the intercalation of cationic surfactant into clay interlayer. Then, the condensation reaction between silane molecule and Si-O tetrahedral sheet of clay (and/or among silane molecules) occurs. The condensation reaction strongly depends on the arrangement of silane molecules within the gallery. For M-2, the arrangement of γ -APS is a parallel-bilayer and the condensation between silane molecules is easy to happen. However, the arrangement of γ -APS in H-2 is a parallel-monolayer. Both of the experimental results [5,18] and our molecular modeling of organoclays indicate that, in the case of parallel-monolayer, the organic molecules or cations within the gallery are individually separated to lower down the energy of the hybrid. Accordingly, there is little possibility for condensation between silane molecules in the case of parallel-monolayer. This could well explain the different T^n ($n=1,2$ and 3) units occurring in M-2 and H-2 as indicated by the ^{29}Si CP/MAS NMR spectra. Figure 6 shows a hypothetical diagram for the intercalation of γ -APS into clay interlayer and silylation of γ -APS onto clay surface, and the possible structural models for T^1 , T^2 and T^3 units.

Our proposed model is different from that reported by Herrera et al. [6] in spite of the similar basal spacing of the grafted products. Herrera et al. [6] suggested that the silane molecules could only react at the “broken” edges of the clay layer rather than with the intra-layer surface. To elucidate this point, the experiment of grafting surfactant-modified-clay (SOMASIF MAE, provided by CO-OP Chemical Co., Japan) with γ -APS was performed. However, the characterization of TGA and ^{29}Si CP/MAS NMR demonstrates that there is no silane grafted onto the organoclay. In addition, molecular dynamics simulation demonstrates that, in organoclays, the alkyl chains within the layer lie almost parallel to the clay surface whereas those out of the layer structure are essentially perpendicular to the surface [19]. This means that the “broken” edge of the clay layer is “protected” by the alkyl chains and there is little possibility for the condensation reaction between the “broken” edges of the clay layer and silane molecules. Our present study has shown that the intercalation of silane molecules into the clay interlayer happens before the condensation between silane molecule and clay layer surface. Hence, we propose that the condensation occurs between silane molecule and the intra-layer surface as shown in Figure 6 rather than between silane molecule and the “broken” edges of the clay layer.

IV. Conclusions

In summary, our present study demonstrates that the grafting reaction between the trifunctional silylating agent and the two 2:1 type layered silicates includes two basic steps: Firstly, the silane molecules are intercalated into the clay interlayer; Then, the condensation reaction happens between silane molecule and clay layer surface. The silane molecules adopt a parallel-bilayer arrangement model in natural montmorillonite (OPTIGEL-757) and a parallel-monolayer arrangement in the synthetic fluorohectorite (ME). The different arrangements of silane molecules in the interlayer result in the various T^n units such as $T^1[\text{Si}(\text{OSi})(\text{OR}')_2\text{R}]$, $T^2[\text{Si}(\text{OSi})_2(\text{OR}')\text{R}]$ and $T^3[\text{Si}(\text{OSi})_3\text{R}]$ during condensation. Consequently, it may leads to the different surface property of the resultant products. This study clearly demonstrates that the interlayer structure of the grafted products and the molecular environment of the grafted silane strongly depend on the used clay materials. It is of high importance in the synthesis of polymer/layered silicate nanocomposites and improvement of their properties.

Acknowledgments

The authors wish to thank Dr. Anne Baudouin for the performance of NMR measurements and Valérie Massardier for technical assistance. The financial supports of Fondation Franco-Chinoise pour Science et ses Applications Académie des Sciences and Fondation Région Rhône-Alpes are gratefully acknowledged.

References

- [1] S. S. Ray, M. Okamoto, *Prog. Polym. Sci.* 28 (2003) 1539.
- [2] G. Lagaly, *Clay Miner.* 16 (1981) 1.
- [3] R. A. Vaia, R. K. Teukolsky, E P. Giannelis, *Chem. Mater.* 6 (1994) 1017.
- [4] L. P. Meier, R. Nueesch, F. T. Madsen, *J. Colloid Interf. Sci.* 238 (2001) 24.
- [5] H. P. He, R. L. Frost, F. Deng, J. X. Zhu, X. Y. Weng, P. Yuan, *Clay Clay Miner.* 52 (2004) 350.
- [6] N. N. Herrera, J. M. Letoffe, J. L. Putaux, L. David, E. Bourgeat-Lami, *Langmuir* 20 (2004) 1564.
- [7] M. Park, I. K. Shim, E. Y. Jung, J. H. Choy, *J. Phys. Chem. Solids* 65 (2004) 499.
- [8] K. Isoda, K. Kuroda, *Chem. Mater.* 12 (2000) 1702.
- [9] A. Shimojima, D. Mochizuki, K. Kuroda, *Chem. Mater.* 13 (2001) 3603.
- [10] K. W. Park, S. Y. Jeong, O. Y. Kwon, *Appl. Clay Sci.* 27 (2004) 21.
- [11] K. C. Vrancken, L. D. Coster, P. V. D. Voort, P. J. Grobet, E. F. Vansant, *J. Colloid Interf. Sci.* 170 (1995) 71.
- [12] J. Duchet, J. F. Gerard, J. P. Chapel, B. Chabert, *J. Adhesion Sci. Technol.*, 14 (2000) 691.
- [13] S. Ek, E. I. Iiskola, L. Niinistö, *J. Phys. Chem. B* 108 (2004) 11454.
- [14] J. X. Zhu, H. P. He, J. G. Guo, D. Yang, X. D. Xie, *Chinese Sci. Bull.* 48 (2003) 368.
- [15] K. A. Carrado, L. Q. Xu, R. Csencsits, J. V. Muntean, *Chem. Mater.* 13 (2001) 3766.
- [16] S. Yariv, *Appl. Clay Sci.* 24 (2004) 225.
- [17] H. P. He, J. G. Guo, X. D. Xie, H. F. Lin, L. Y. Li, *Clay Miner.* 37 (2002) 323.
- [18] Y. Q. Li, H. Ishida, *Langmuir* 19 (2003) 2479.
- [19] Q. H. Zeng, A. B. Yu, G. Q. Lu, R. K. Standish, *J. Phys. Chem. B* 108 (2004) 10025.

Figure captions

Figure 1 Idealized structure of 2:1 type layered silicate. (top: stick and ball style; bottom: polyhedron style.)

Figure 2 FTIR spectra ($2500\text{--}4000\text{ cm}^{-1}$) of natural montmorillonite (M-0) and synthetic fluorohectorite (H-0) before and after grafting.

Figure 3 XRD patterns of natural montmorillonite (M-0) and synthetic fluorohectorite (H-0) before and after grafting.

Figure 4 TGA and DTG curves of natural montmorillonite (M-0) and synthetic fluorohectorite (H-0) before and after grafting.

Figure 5 ^{29}Si MAS NMR spectra of natural montmorillonite (M-0) and synthetic fluorohectorite (H-0) before and after grafting.

Figure 6 The hypothetical diagram for the intercalation and silylation of γ -APS into clay interlayer, and the possible structural models for T^1 , T^2 and T^3 units.

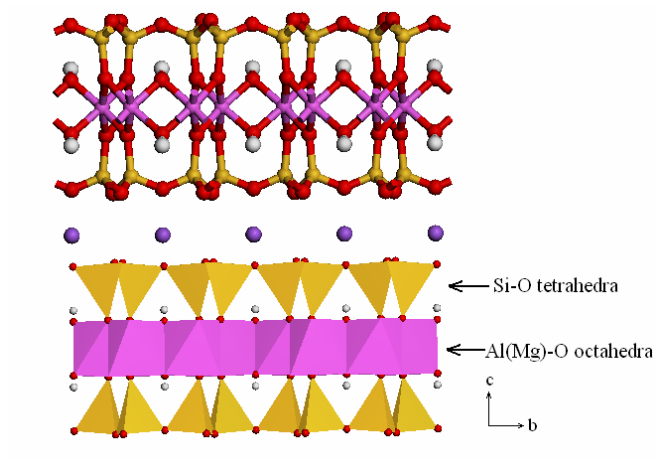


Figure 1

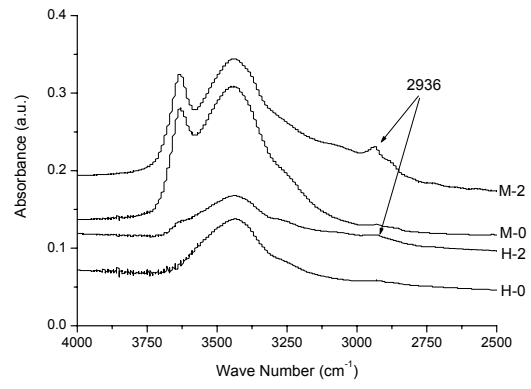


Figure 2

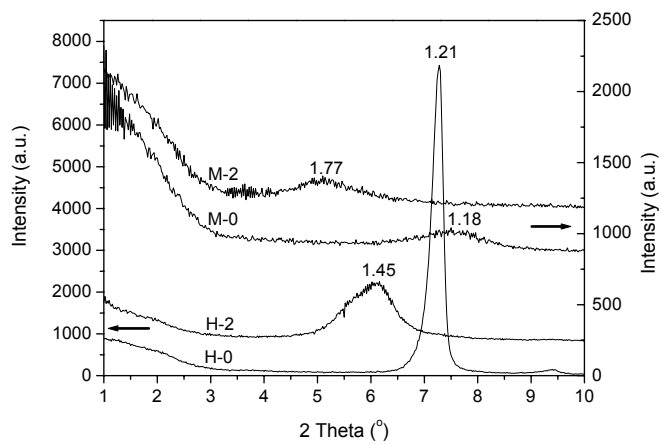


Figure 3

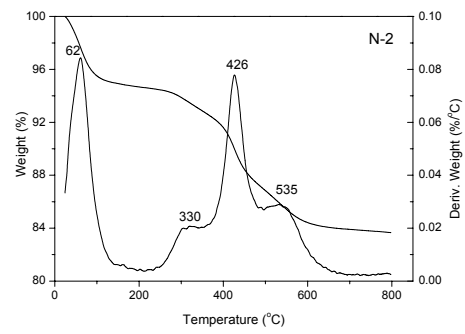
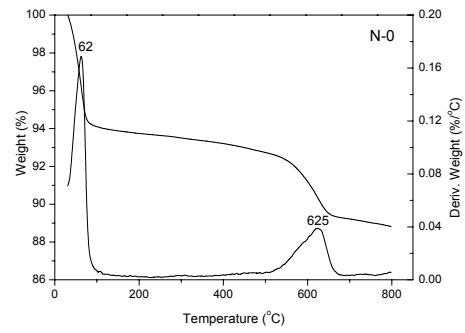
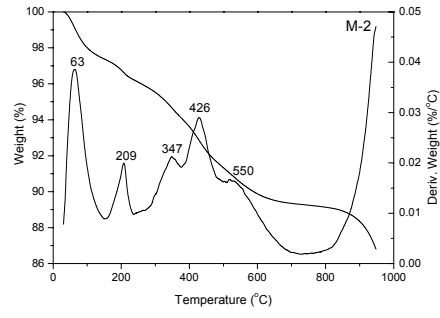
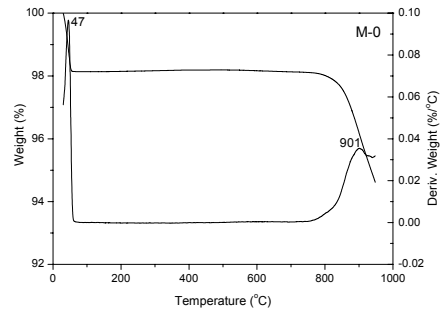


Figure 4

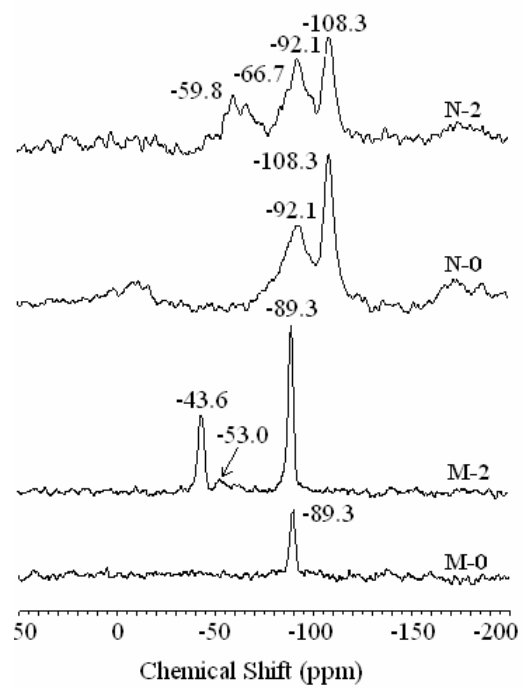


Figure 5

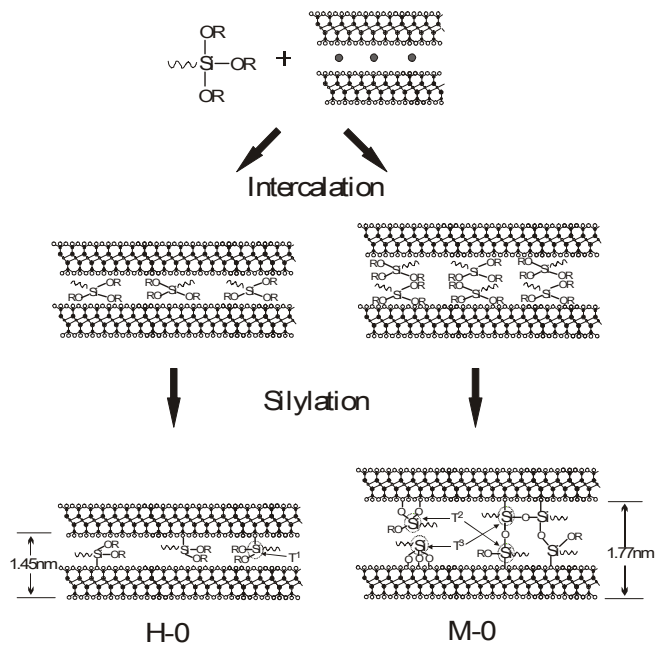


Figure 6